

Statistical Methods for Image Segmentation

Sridhar Lakshmanan
*University of Michigan —
 Dearborn*

1	Introduction.....	443
2	Image Segmentation: The Mathematic Problem	445
3	Image Statistics for Segmentation	445
	3.1 Gaussian Statistics • 3.2 Fourier Statistics • 3.3 Covariance Statistics	
	3.4 Label Statistics	
4	Statistical Image Segmentation	446
	4.1 Vehicle Segmentation • 4.2 Aerial Image Segmentation	
	4.3 Segmentation for Image Compression	
5	Discussion	451
	References	452

1 Introduction

Segmentation is a fundamental low-level operation on images. If an image is already partitioned into segments, where each segment is a “homogeneous” region, then a number of subsequent image processing tasks become easier. A homogeneous region refers to a group of connected pixels in the image that share a common feature. This feature could be brightness, color, texture, motion, etc. (Fig. 1). References 1–5 contain exploratory articles on image segmentation, and they provide an excellent place to start for any newcomer researching this topic.

Boundary detection is the dual goal of image segmentation. After all, if the boundaries between segments are specified then it is equivalent to identifying the individual segments themselves. However, there is one important difference. In the process of image segmentation, one obtains region-wise information regarding the individual segments. This information can then be subsequently used to classify the individual segments. Unfortunately, detection of the boundaries between segments does not automatically yield region-wise information about the individual segments. So, further image analysis is necessary before any segment-based classification can be attempted. Since segmentation, and not classification, is the focus of this chapter, from here on image segmentation is meant to include the dual problem of boundary detection

as well. Note that boundary detection is distinctly different from edge detection. Edges are typically detected by examining the local variation of image intensity or color. Edge detection is covered in three separate Chapters, 4.14, 4.1.5, and 4.18.

The importance of segmentation is clear by the central role it plays in a number of applications that involve image and video processing — remote sensing, medical imaging, intelligent vehicles, video compression, etc. The success or failure of segmentation algorithms in any of these applications is heavily dependent on the type of feature(s) used,¹ the reliability with which these features are extracted, and the criteria used for merging pixels based on the similarity of their features.

As one can gather from references 1–5 there are many ways to segment an image. So, the question is, why statistical methods? Statistical methods are a popular choice for image segmentation because they involve image features that are simple to interpret by using a model, features that are easy to compute from a given image, and merging methods that are firmly rooted in statistical/mathematic inference — see Chapters 4.3, 4.5, 4.7, and 10.10 for various examples. While there is no explicit consensus in the image processing community that statistical methods are the way to go as far image segmentation is concerned, the volume and diversity of

¹Features refer to image attributes such brightness, color, texture, motion, etc.

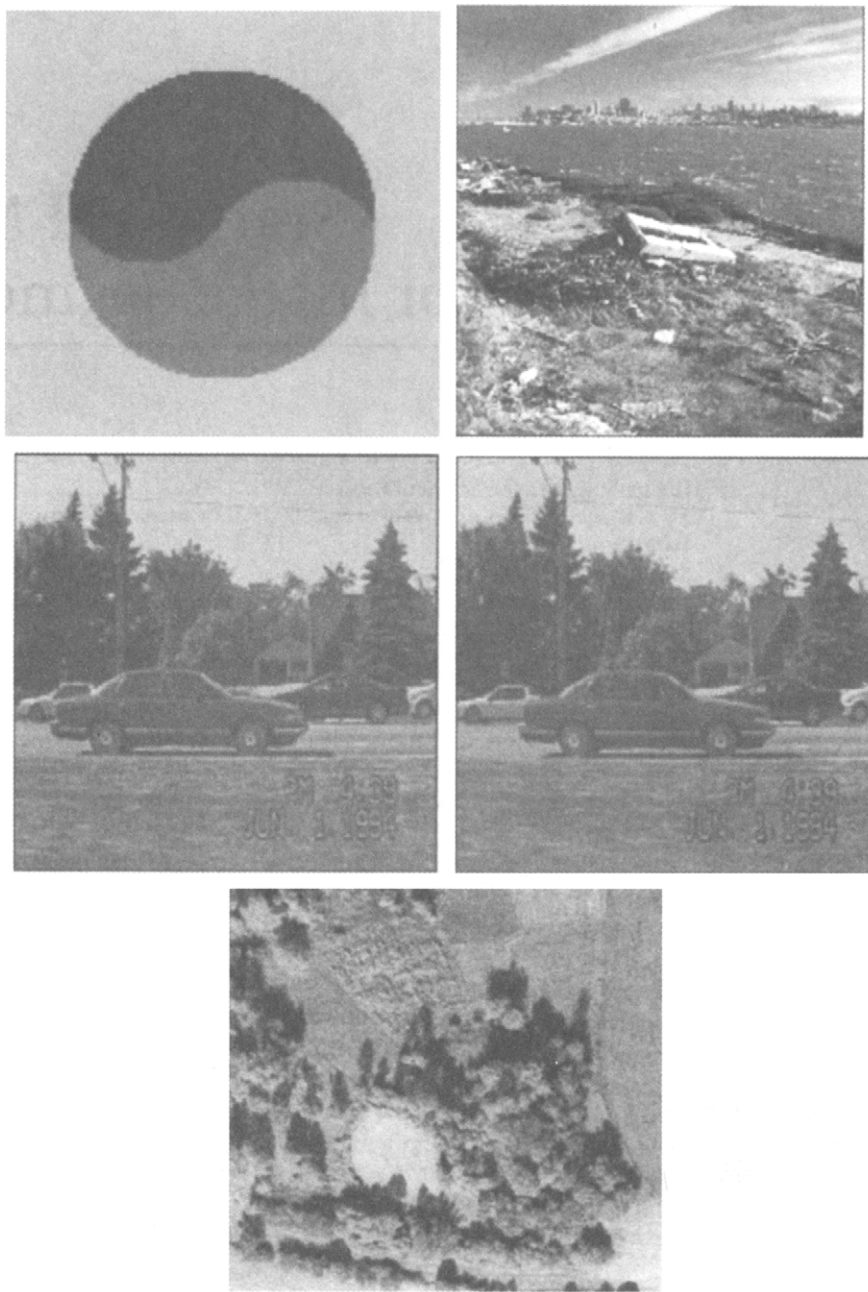


FIGURE 1 Examples of images that could be segmented based on brightness (top left), color (top right), motion (middle row), and texture (bottom row).

publications certainly seem to indicate they are a very popular choice. An example serves to illustrate the point. Consider the images in Fig. 2. It is clear that each of these images consists of 4 homogenous regions delineated by spatially contiguous boundaries, and pixels belonging to each region share a common texture. So the question becomes, how does one represent/identify/model the spatial continuity/relationship that exists between pixels that share a common texture? This is not a trivial question, because two blocks of pixels from two entirely different parts of the image may exhibit the same type

of distribution² that makes them indistinguishable. On the other hand, if one examines statistics other than the block mean and variance the textural differences between pixels belonging to those two blocks become more apparent. The rest of this chapter is devoted to describing a handful of these “other” statistics and their role in image segmentation.

²For example, the blocks may have the same average pixel intensity values (means) and spread of intensity values about the mean (variances).

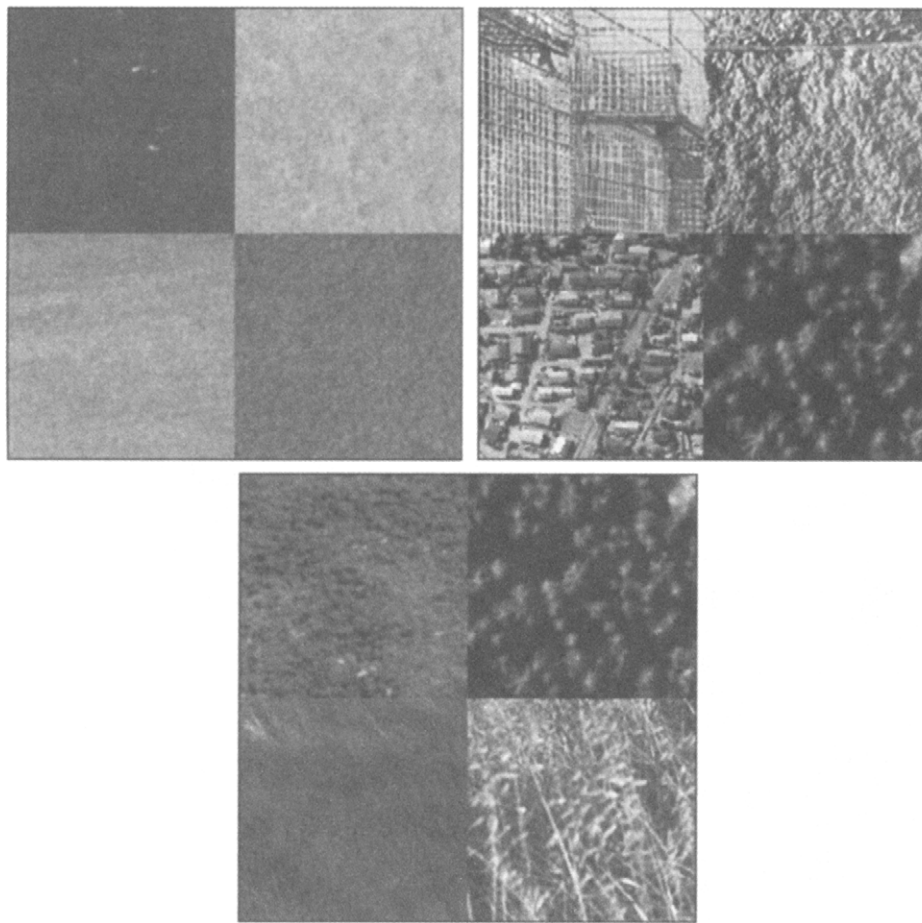


FIGURE 2 Collection of images; in each there are four clearly distinguishable segments. (See color insert.)

2 Image Segmentation: The Mathematic Problem

Let $\Omega = \{(m, n) : 1 \leq m \leq M \text{ and } 1 \leq n \leq N\}$ denote an $M \times N$ lattice of points (m, n) . An observed image f is a function defined on this domain Ω , and for any given point (m, n) the observation $f(m, n)$ at that point takes a value from a set Λ . Two common examples for the set Λ are: $\Lambda = \{\lambda : 0 \leq \lambda \leq 255\}$ for black-white images, and $\Lambda = \{(\lambda_1, \lambda_2, \lambda_3) : 0 \leq \lambda_1 \leq 255, 0 \leq \lambda_2 \leq 255, \text{ and } 0 \leq \lambda_3 \leq 255\}$ for color (red, green, and blue channel) images. A segmented image g is also a function on the same domain Ω , but for any given point (m, n) the segmentation $g(m, n)$ at that point takes a value from a different set Γ . Two common examples for the set Γ are: $\Gamma = \{\gamma : \gamma = 0 \text{ or } 1\}$ denoting the two segments in a binary segmentation, and $\Gamma = \{\gamma : \gamma = 1, 2, 3, 4, \dots, k\}$ denoting the k different segments in the case of a multi-class segmentation. Of course, g could also denote a boundary image. For any given point (m, n) , $g(m, n) = 1$ could denote the presence of a boundary at that point and $g(m, n) = 0$ the absence.

Given a particular realization of the observed image $f = f_0$, the problem of image segmentation is one of estimating the corresponding segmented image using $g_0 = h(f_0)$. Statistical methods for image segmentation provide a coherent derivation of this estimator function $h(\cdot)$.

3 Image Statistics for Segmentation

To understand the role of statistics in image segmentation, it pays to examine some preliminary functions that operate on images. Given an image f_0 that is observed over the lattice Ω , suppose that $\Omega_1 \subseteq \Omega$ and f_1 is a restriction of f_0 to only those pixels that belong to Ω_1 . Then, one can define a variety of statistics that capture the spatial continuity of the pixels that comprise f_1 . Here are some common examples:

3.1 Gaussian Statistics

$$T_{f_1}(p, q) = \sum_{(m, n) \in \Omega_1} [f_1(m, n) - f_1(m + p, n + q)]^2,$$

for $(p, q) \in \{(0, 1), (1, 0), (1, 1), (1, -1), \dots\}$ (1)

measures the amount of variability in the pixels that comprise f_1 along the (p, q) th direction. For a certain, f_1 , if $T_{f_1}(0, 1)$ is very small, for example, then that implies that f_1 has a little or no variability along the $(0, 1)$ th (i.e., horizontal) direction. Computation of this statistic is straightforward as it is merely a quadratic operation on the difference between intensity values of adjacent (neighboring) pixels. $T_{f_1}(p, q)$ and minor variation thereof is referred to as the Gaussian statistic and is widely used in statistical methods for segmentation of gray-tone images [6, 7].

3.2 Fourier Statistics

$$F_{f_1}(\alpha, \beta) = \sum_{(m, n) \in \Omega_1} \left[f_1(m, n) e^{-\sqrt{-1}(m\alpha+n\beta)} \right] \\ \times \left[f_1(m, n) e^{\sqrt{-1}(m\alpha+n\beta)} \right], \quad \text{for } (\alpha, \beta) \in [-\pi, \pi]^2 \quad (2)$$

measures the amount of energy in frequency bin (α, β) that the pixels that comprise f_1 possess. For a certain f_1 , if $F_{f_1}(0, 20\pi/N)$ has a large value, for example, then that implies that f_1 has a significant cyclical variation along the $(0, 20\pi N)$ th (i.e., horizontally every 10 pixels) frequency. Computation of this statistic is more complicated than the Gaussian one. The use of fast Fourier transform algorithms, however, can significantly reduce the associated burden. $F_{f_1}(\alpha, \beta)$, called the periodogram statistic, is also used in statistical methods for segmentation of textured images [8, 9].

3.3 Covariance Statistics

$$K_{f_1} = \sum_{(m, n) \in \Omega_1} (f_1(m, n) - \mu_{f_1})^T (f_1(m, n) - \mu_{f_1}), \quad \text{where} \\ \mu_{f_1} = \sum_{(m, n) \in \Omega_1} f_1(m, n) \quad (3)$$

measures the correlation between the various components that comprise each pixel of f_1 . If K_{f_1} is a 3×3 matrix and $K_{f_1}(1, 2)$ has large value, for example, then that means that components 1 and 2 (could be the red and green channels) of the pixels that make up f_1 are highly correlated. Computation of this statistic is very time consuming, even more so than the Fourier one, and there are no known methods to alleviate this burden. K_{f_1} is called the covariance matrix of f_1 , and this too has played a substantial role in statistical methods for segmentation of color images [10, 11].

3.4 Label Statistics

$$L_{g_1}(m, n) = \Psi[g_1(m, n), g_1(m + p, n + q)], \quad \text{where} \\ \Psi(a, b) = \begin{cases} 1, & \text{if } a = b \\ -1, & \text{if } a \neq b \end{cases} \\ \text{for } (p, q) \in \{(0, 1), (1, 0), (1, 1), (1, -1), \dots\} \quad (4)$$

measures the amount of homogeneity in the pixels that comprise g_1 along the (p, q) th direction. For a certain g_1 , if $L_{g_1}(1, 1)$ is very large, for example, then that implies that g_1 has a little or no variability along the $(1, 1)$ th (i.e., 135 degrees diagonal) direction. Computation of this statistic is straightforward, as it is merely an indicator operation on the difference between label values of adjacent (neighboring) pixels. $L_{g_1}(p, q)$ and minor variation thereof is referred to as the label statistic and is widely used in statistical methods for restoration of gray-tone images [12, 13].

4 Statistical Image Segmentation

Computation of image statistics of the type defined in Section 3 tremendously facilitates the task of image segmentation. To illustrate their utility, three image segmentation problems that arise in three distinctly different applications are presented below. In each case, a description of the how a solution was arrived at using statistical methods is given.

4.1 Vehicle Segmentation

Today, there is a desire among consumers worldwide for automotive accessories that make their driving experience safer and more convenient. Studies have shown that consumers believe that safety and convenience accessories are important in their new car purchasing decision. In response to this growing market, the automotive industry in cooperation with government agencies has embarked on programs to develop new safety and convenience technologies. These include, but are not limited to, collision warning (CW) systems, lane departure warning (LDW) systems, and intelligent cruise control (ICC) systems. These systems and others comprise an area of study referred to as intelligent transportation systems (ITS), or more broadly, intelligent vehicle highway systems (IVHS).

An important image segmentation problem within ITS is one of segmenting vehicles from their background [14].



FIGURE 3 Typical image in which a vehicle has to be segmented from the background.

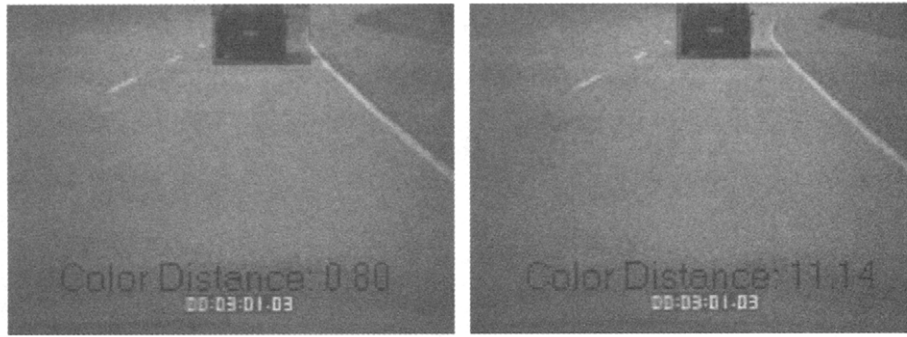


FIGURE 4 Fisher color distance between pixels inside and outside of a square template placed on top of the image in Fig. 3. The template hypothesis on the right has higher merit than the one on the left.

Figure 3 contains a typical image where a vehicle needs to be segmented from its background. In the following paragraphs, a statistical method for this segmentation is described. The vehicle of interest, it is assumed,³ is merely a square that is described by three parameters (V_b , V_l , V_w) corresponding to the bottom, left edges, and width of the square. Different values of these three parameters yield vehicles of different sizes and positions within the image.

When seen from their rear, vehicles seldom appear in the image too big or small,⁴ and so depending on the distance of the vehicle from the camera it is possible to expect that the width of the vehicle to be within a certain range. Suppose that W_{\min} and W_{\max} denote this range, then

$$P(V_w) = \begin{cases} 1/(W_{\max} - W_{\min}), & \text{if } W_{\min} \leq V_w \leq W_{\max} \\ 0, & \text{otherwise} \end{cases} \quad (5)$$

is a probability density function (pdf) that enforces the strict constraint that V_w , be between W_{\min} and W_{\max} . Since it is a probability over (one of) the quantities being estimated it is commonly referred to as a prior pdf, or simply a prior.

Let (v_b, v_l, v_w) denote a specific hypothesis of the unknown vehicle parameters (V_b, V_l, V_w) . The merit of this hypothesis is decided by another probability called the likelihood pdf, or simply the likelihood. In this application, it is appealing to decide the merit of a hypothesis by evaluating the difference in color between pixels that are inside the square (i.e., the pixels that are hypothesized to be the vehicle) and those that immediately surround the square (i.e., the pixels that are in the immediate background of the hypothesized vehicle). The specific color difference evaluator that is employed is called the Fisher distance:

$$\text{FishDist}(v_b, v_l, v_w) = (\mu_1 - \mu_2)^T (K_1 + K_2)^{-1} (\mu_1 - \mu_2), \quad (6)$$

³This is a valid assumption when the rear-view of the vehicle is obtained from a camera placed at groundlevel.

⁴Even accounting for the variations in the actual physical dimensions of the vehicle.

where μ_1 and K_1 are the mean and covariance of the pixels that are inside the hypothesized square — computed by using Eq. (3) — and μ_2 and K_2 are the mean and covariance of pixels that are immediately surrounding the hypothesized square. Hypotheses corresponding to a large color difference between pixels inside and immediately surrounding the square have more merit (and hence a higher probability of occurrence) than those with smaller color difference (Fig. 4).

The problem of segmenting a vehicle from its background boils down to estimating the three parameters (V_b, V_l, V_w) from the given color image. An “optimal”⁵ estimate of these parameters is the one that maximizes the product of the prior and likelihood probabilities in Eqs. (5) and (6), respectively — the so-called maximum *a posteriori* (MAP) estimate. Figure 5 shows a few examples of estimating the correct (V_b, V_l, V_w) using this procedure. This same procedure can also be adapted to segment images in other applications. Figure 6 shows a few examples where the procedure has been used to segment images that are entirely different from those in Figs. 3–5.

4.2 Aerial Image Segmentation

Accurate maps have widespread uses in modern day-to-day living. Maps of urban and rural areas are regularly used in an entire spectrum of civilian and military tasks starting from simple ones like obtaining driving directions all the way to complicated ones like highway planning. Maps themselves are just a portion of the information, and are typically used to index other important geophysical attributes such as weather, traffic, population, size, etc. Large systems called geographical information systems (GIS) collate, maintain, and deliver maps, weather, population, etc., on demand.

Image segmentation is a tool that finds widespread use in the creation and maintenance of GIS. One example pertains to the operator-assisted updating of old maps using aerial images, where segmentation is used to supplement/complete the human operator [15]. Shown in Fig. 7 is an aerial

⁵Optimal in the sense that among all estimates of the parameters, the one that minimizes the probability of making an error.



FIGURE 5 Correct estimation of the vehicle ahead, using the MAP procedure. (See color insert.)

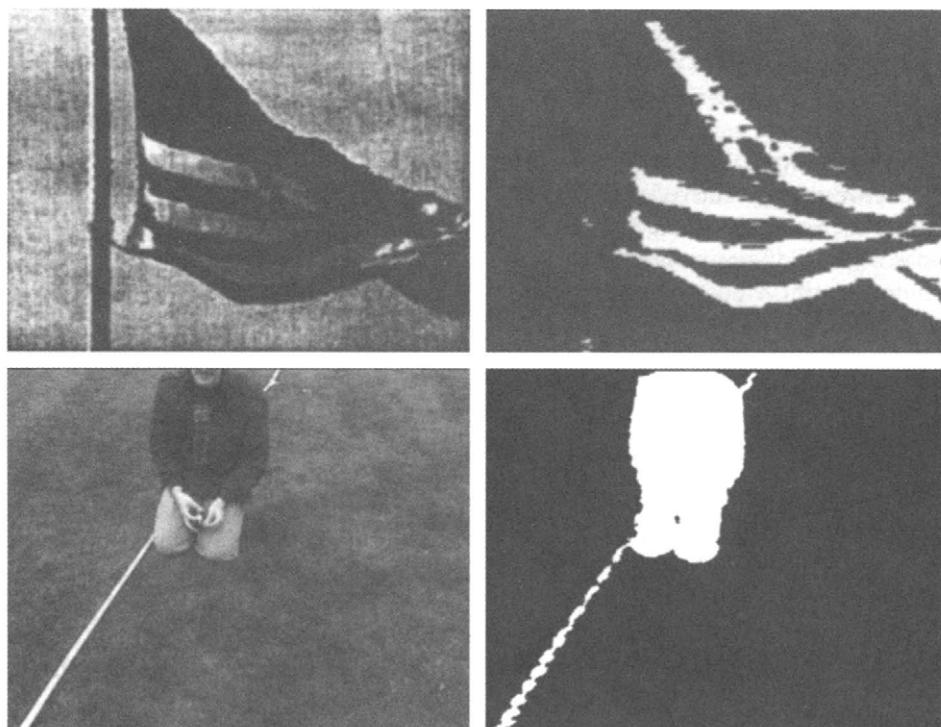


FIGURE 6 Segmentation of other images, using the same Fisher color distance. Top: A segmentation that yields all segments that contain the color white. Bottom: A segmentation that yields all segments that do not contain the color green. (See color insert.)

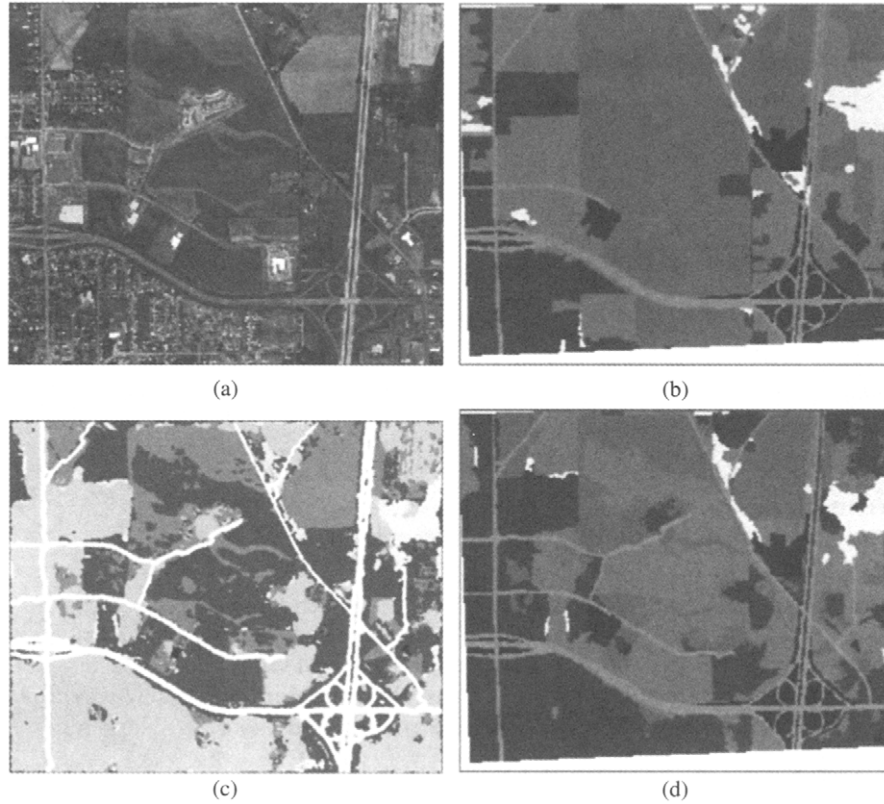


FIGURE 7 Updating old maps using image segmentation. (a) Aerial image of Eugene, Oregon in 1993. (b) Map of the same area in 1987. (c) Operator-assisted segmentation of the 1993 aerial image. (d) Updated map in 1993. (See color insert.)

image of the Eugene, Oregon, area taken in 1993. Accompanying the aerial image is an old (1987) map of the same area that indicates what portion of that area contains brown crops (in red), grass (in green), development (in blue), forest (in yellow), major roads (in gray), and everything else (in black). The aerial image indicates a significant amount of change in the area's composition from the time the old map was constructed. Especially noticeable is the new development of a road network south of the highway, in an area that used to be a large brown field of crops. The idea is to use the new 1993 aerial image in order to update/correct the old 1987 map. The human operator examines the aerial image and chooses a collection of polygons corresponding to various homogeneous segments of the image. Using the pixels with these polygons as a training sample, a statistical segmentation of the aerial image is effected — the segmentation result is also shown in Fig. 7. Regions in the old map are compared to segments of the new image, and where they are different, the old map is updated/corrected — the resulting new map is shown in Fig. 7 as well.

The segmentation procedure used for this map updating application is based on Gaussian statistics — see Eq. (1). Specifically, for each homogeneous polygonal region selected in the aerial image by the human operator, the Gaussian statistics for that polygon are automatically computed. Using

these statistics, a model of probable variation in the pixels' intensities within the polygon is subsequently created:⁶

$$P(f_l|\theta_l) = \frac{1}{Z(\theta_l)} \exp \left\{ - \sum_{p,q} T_{f_l}(p,q) \theta_l(p,q) \right\}, \quad (7)$$

where f_l denotes the pixels within the l th polygon, $Z(\theta_l)$ is a normalizing constant that makes $\sum_{f_l} P(f_l|\theta_l) = 1$, and $\theta_l(p, q)$ are parameters chosen so that $P(f_l|\theta_l) \geq P(f_l|\phi)$ for all $\phi \neq \theta_l$. Eq. (7) forms the basis for segmenting the aerial image in Fig. 7. Suppose that there are k distinctly different polygonal segment — corresponding to k distinctly different θ_l values — then each pixel (m, n) in the aerial image is classified according to a maximum likelihood rule. The probability of how likely $f(m, n)$ is if it were classified as belonging to the l th is assessed according to Eq. (7), and the pixel is classified as belonging to class l if $P(f(m, n)|\theta_l) \geq P(f(m, n)|\theta_r)$ for all $r \neq l$. Shown in Fig. 8 is another example of segmenting an aerial image using this same maximum likelihood statistical procedure.

⁶This model is referred to as the Gaussian Markov random field model [6–9].

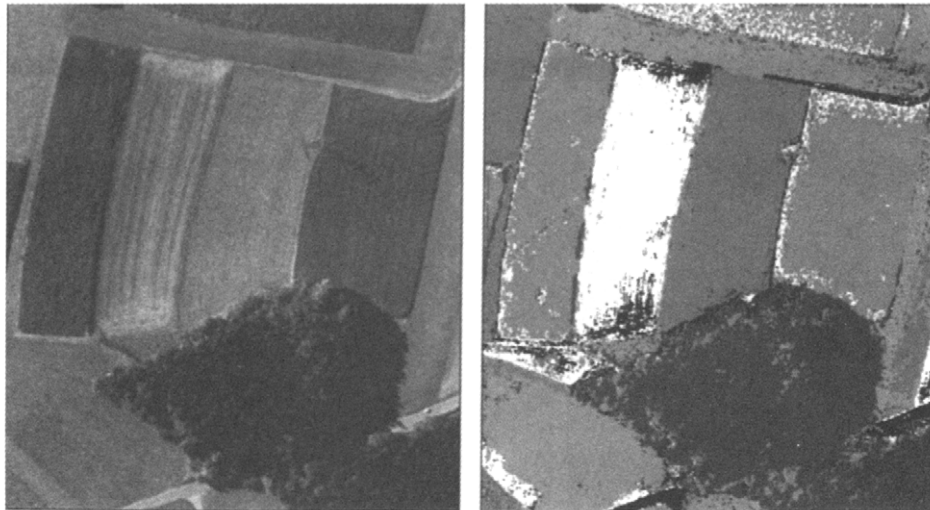


FIGURE 8 Segmentation of another aerial image, this time of a rural crop field area, using the same texture-based maximum likelihood procedure employed in Fig. 7. (See color insert.)

4.3 Segmentation for Image Compression

The enormous amount of image and video data that typifies many modern multimedia applications mandates the use of encoding techniques for their efficient storage and transmission.

The use of such encoding is standard in new personal computers, video games, digital video recorders/players/disks, digital television, etc. Image and video encoding schemes that are “object-based” are most efficient (i.e., achieve the best compression rates), and also facilitate many advanced

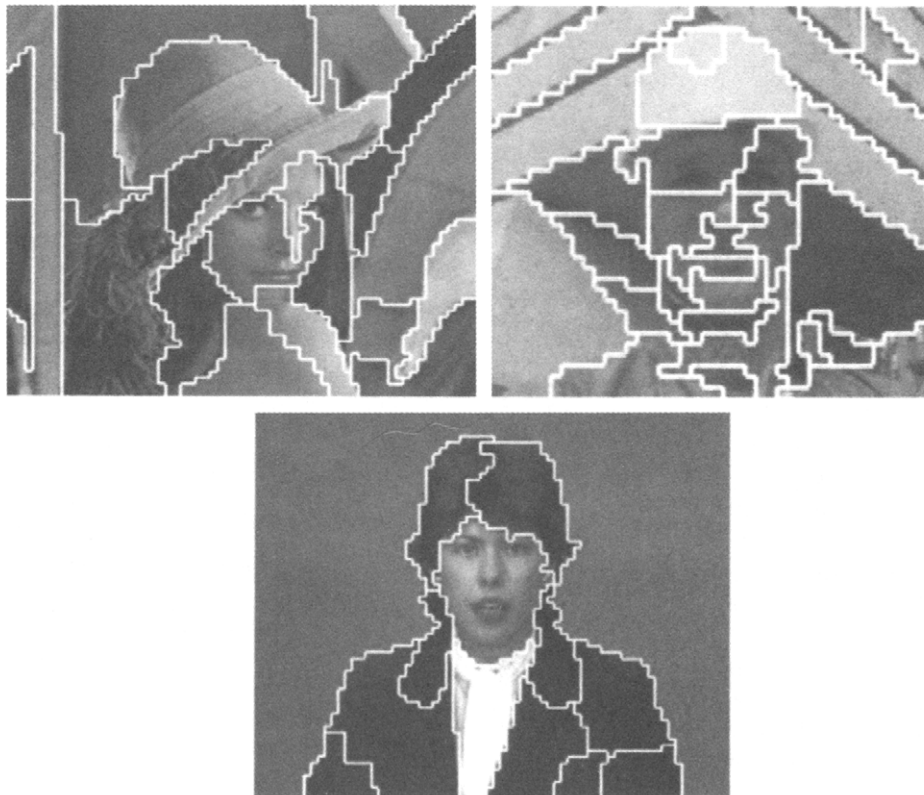


FIGURE 9 Block-based segmentation of images into large “homogeneous” objects, using a MAP estimation method that employs Fourier statistics.

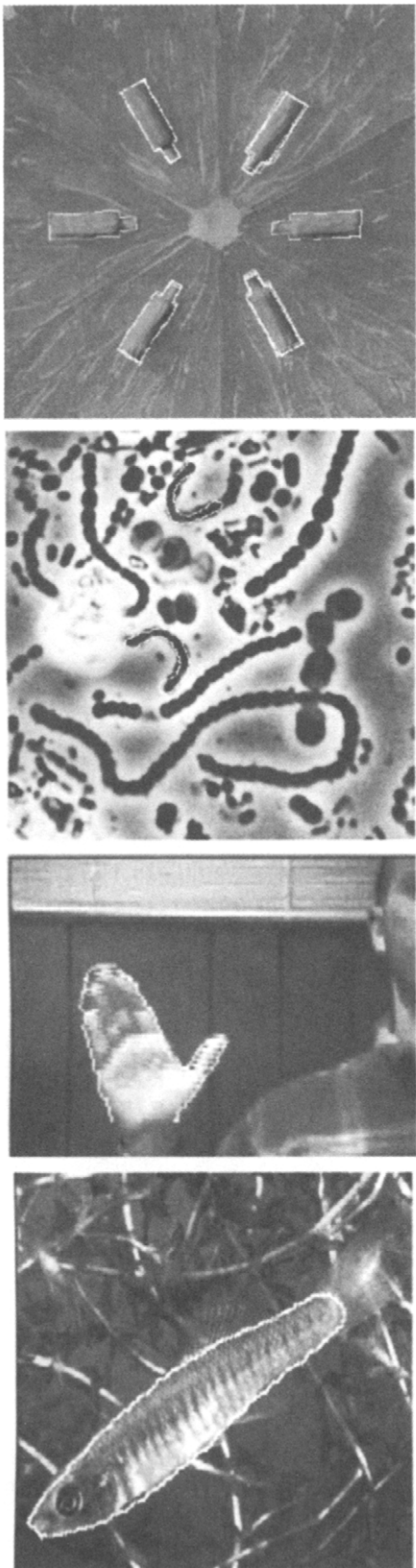


FIGURE 10 Segmenting objects out of images when they “resemble” the query.

multimedia functionalities. Object-based encoding of images and video, however, require that the objects be delineated *a priori*. An obvious method for extracting objects in an image is by segmenting it.

Reference 16 describes a statistical image segmentation method that is particularly geared for object-based encoding of images and video. A given image is first divided into 8×8 blocks of pixels, and for each block, the Fourier statistics of the pixels in that block is computed. If the pixels f_1 within a single block have little or no variation, then $F_{f_1}(0, 0)$ will have a very large value; similarly, if the block contains a vertical edge, then $\sum_\beta F_{f_1}(0, \beta)$ will have a very large value, and so on. There are six such categories, corresponding to uniform/monotone, vertical edge, horizontal edge, 45-degree diagonal edge, 135-degree diagonal edge, and texture (randomly oriented edge). Let $t_{f_1}(1), t_{f_1}(2), \dots, t_{f_1}(6)$, be the Fourier statistics-based quantities — one of their values will be large corresponding to which of these six categories f_1 belongs.

If g denotes the collection of unknown block labels, then an estimate of g from f would correspond to an “object-based” segmentation of f . Reference 16 pursues a MAP estimate of g from f , where the prior pdf



$$P(g = g_0) = \frac{1}{Z} \exp \left\{ - \sum_{p, q} L_{g_0}(p, q) \right\}, \quad (8)$$

and the likelihood pdf

$$P(f = f_0 | g = g_0) = \frac{1}{C(g_0)} \exp \left\{ - \sum_{m, n} t_{f_{m, n}}(g_0(m, n)) \right\}. \quad (9)$$

Where Z and $C(g_0)$ are the normalizing constants for the prior and the likelihood pdf's, respectively, the index (m, n) denotes the 8×8 blocks, and $L_g(p, q)$ is the label statistic defined in eq. (4). Figure 9 shows a few examples of image segmentation using this procedure.

5 Discussion

The previous four sections provide a mere sampling of the various statistical methods that are employed for image segmentation; see Ref. 21 for an epistemological summary. References [17–20, 22] contain some of the other methods. The main differences between those and the methods described in this chapter lie in the type of prior and/or likelihood pdfs employed.

In particular, [20] contains a method for image segmentation that is based on elastic deformation of templates. Rather than specify a prior pdf as probability over the space of all images, [20] specifies a prior pdfs over the space of all deformations of a prototypical image. The space of deformations of the prototype image is a very rich one and even

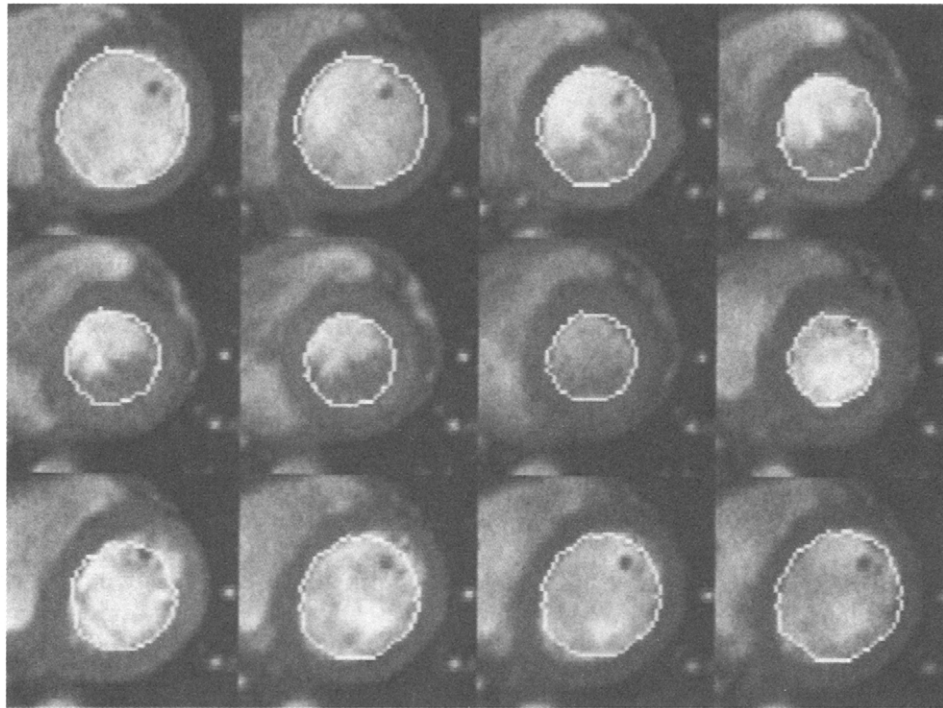


FIGURE 11 Tracking an object of interest, in this case a human heart, from frame to frame by using the elastic deformation method described in [20].

includes images that are quite distinctly different from the original. More importantly, the deformation space's dimension is significantly smaller than the conventional space of all images that "resemble" the prototype. This smaller dimension pays tremendous dividends when it comes to image segmentation.

Query of image databases provides an important application where a prototype of an object to be segmented from a given image is readily available. A user may provide a typical object of interest — its approximate shape, color and texture — and ask to retrieve all database images that contain objects similar to the one of interest. Figure 10 shows a few examples of the object(s) of interest being segmented out of a given image by using the elastic deformation method described in [20]. Figure 11 shows an example of tracking an object from frame-to-frame using the same method.

As one can gather from this chapter, when statistical methods are employed for image segmentation, there is always an associated multivariate optimization problem. The number of variables involved in the problem varies according to the dimensionality of the prior pdf's domain space. For example, the MAP estimation procedure in the vehicle segmentation application has an associated three-parameter optimization problem. Whereas the MAP estimation procedure in the segmentation for image compression application, has an associated 64×64 parameter optimization problem. The functions that need to be maximized with respect to these

variables are typically non-concave, and contain many local maxima. This implies that simple gradient-based optimization algorithms cannot be employed, as they are prone to converge to a local (as opposed to the global) maxima. Statistical methods for image segmentation abound with a wide variety of algorithms to address such multivariate optimization problems. The reference list that follows this section contains several distinct examples: [12] contains the greedy iterated conditional maximum (ICM) algorithm; [9, 13, 18] contain a stochastic algorithm called Gibbs sampler (a simulated annealing procedure); [2] contains a randomized jump-diffusion algorithm; [20] contains a multi-resolution algorithm; [23] contains an evolutionary algorithm; and finally [24] contains a Markov chain Monte Carlo algorithm. For a given application, there always appears to be a "most appropriate" algorithm, although any of the existing global optimization algorithms can conceptually be employed.

References

- [1] D. Geiger and A. Yuille. A common framework for image segmentation. *Int. J. Comput. Vision*, 6(3), 227–243, 1990.
- [2] U. Grenander and M. I. Miller. Representation of knowledge in complex systems. *J. Royal Statistical Society (B)*, 56(30), 1–33, 1994.
- [3] M. J. Swain and D. H. Ballard. Color Indexing. *Int. J. Comput. Vision*, 7(1), 11–32, 1991.

- [4] T. R. Reed and J. M. H. Du Buf. A review of recent texture segmentation and feature extraction techniques. *Comput. Vision, Graphics and Image Process. — Image Understanding*, 57(3), 359–372, 1993.
- [5] H.-H. Nagel. Overview on image sequence analysis. In T. S. Huang, editor, *Image Sequence Processing and Dynamic Scene Analysis*, pp. 2–39. Springer-Verlag, 1983.
- [6] J. Zhang. Two-Dimensional Stochastic Model-Based Image Analysis. Ph. D. Thesis. Rensselaer Polytechnic Institute, Troy, NY, 1988.
- [7] C.-S. Won and H. Derin. Unsupervised segmentation of noisy and textured images using Markov random field models. *Comput. Vision, Graphics and Image Process. — Graphical Models and Image Processing*, 54(4), 308–328, 1992.
- [8] R. Chellappa. Two-dimensional discrete Gaussian Markov random fields for image processing. In L. N. Kanal and A. Rosenfeld, editors, *Progress in Pattern Recognition: Vol. 2*, North-Holland, 1985.
- [9] F. C. Jeng and J. W. Woods. Compound Gauss-Markov random fields for image estimation. *IEEE Trans. Signal Processing*, 39, 683–691, 1991.
- [10] D. Panjwani and G. Healy. Markov random fields for unsupervised segmentation of textured color images. *IEEE Trans. Pattern Analysis and Machine Intelligence*, 17(10), 939–954, 1995.
- [11] A. C. Hurlbert. *The Computation of Color*. Ph. D. Thesis. Massachusetts Institute of Technology, Cambridge, MA, 1989.
- [12] J. E. Besag. On the statistical analysis of dirty pictures. *J. Royal Statistical Society (B)*, 48, 259–302, 1986.
- [13] S. Geman and D. Geman. Stochastic relaxation, Gibbs distributions, and the Bayesian restoration of images. *IEEE Trans. Pattern Analysis and Machine Intelligence*, 6, 721–741, 1984.
- [14] M. Beauvais and S. Lakshmanan. CLARK: A heterogeneous sensor fusion method for finding lanes and obstacles. *Image Vision Computing*, 18(5), 397–413, 2000.
- [15] M.-P. Dubuisson Jolly and A. Gupta. Color and Texture Fusion: Application to aerial image segmentation and GIS updating. *Proceedings of the 3rd IEEE Workshop on Applications of Computer Vision*, 2–7, 1996.
- [16] C. S. Won. A block-based MAP segmentation for image compressions, *IEEE Trans. Circuit and System for Video Technology*, 8(5), 592–601, 1998.
- [17] R. Chellappa and A. K. Jain (editors). *Markov Random Fields: Theory and Application*. Academic Press, 1992.
- [18] D. Geman and G. Reynolds. Constrained restoration and the recovery of discontinuities. *IEEE Trans. Pattern Analysis and Machine Intelligence*, 14, 367–383, 1992.
- [19] D. Keren, D. B. Cooper, and J. Subrahmonia. Describing complicated objects by implicit polynomials. *IEEE Trans. Pattern Analysis and Machine Intelligence*, 16(1), 38–53, 1994.
- [20] Y. Zhong. *Object Matching Using Deformable Templates*. Ph. D. Thesis. Michigan State University, East Lansing, MI 1997.
- [21] S.-C. Zhu. Statistical modeling and conceptualization of visual patterns. *IEEE Trans. Pattern Analysis and Machine Intelligence*, 25(6), 691–712, 2003.
- [22] M. W. Woolrich, T. E. J. Behrens, C. F. Beckmann, and S. M. Smith. Mixture models with adaptive spatial regularization for segmentation with an application to fMRI data. *IEEE Trans. Medical Imaging*, 24(1), 1–11, 2005.
- [23] X. Wang and H. Wang. Evolutionary optimization with Markov random field prior. *IEEE Trans. Evolutionary Computation*, 8(6), 567–579, 2004.
- [24] Z. Tu and S.-C. Zhu. Image segmentation by data-driven Markov chain Monte Carlo. *IEEE Trans. Pattern Analysis and Machine Intelligence*, 24(5), 657–673, 2002.



FIGURE 4.6.11 Original Lena.

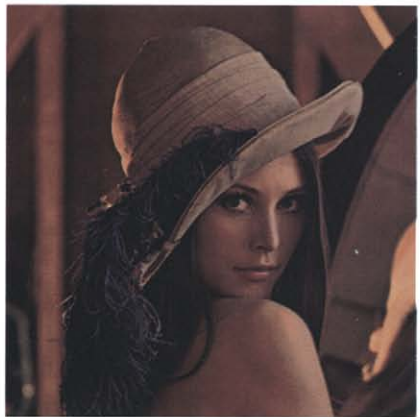


FIGURE 4.6.12 Calibrated Lena.



FIGURE 4.6.13 New scan of Lena.

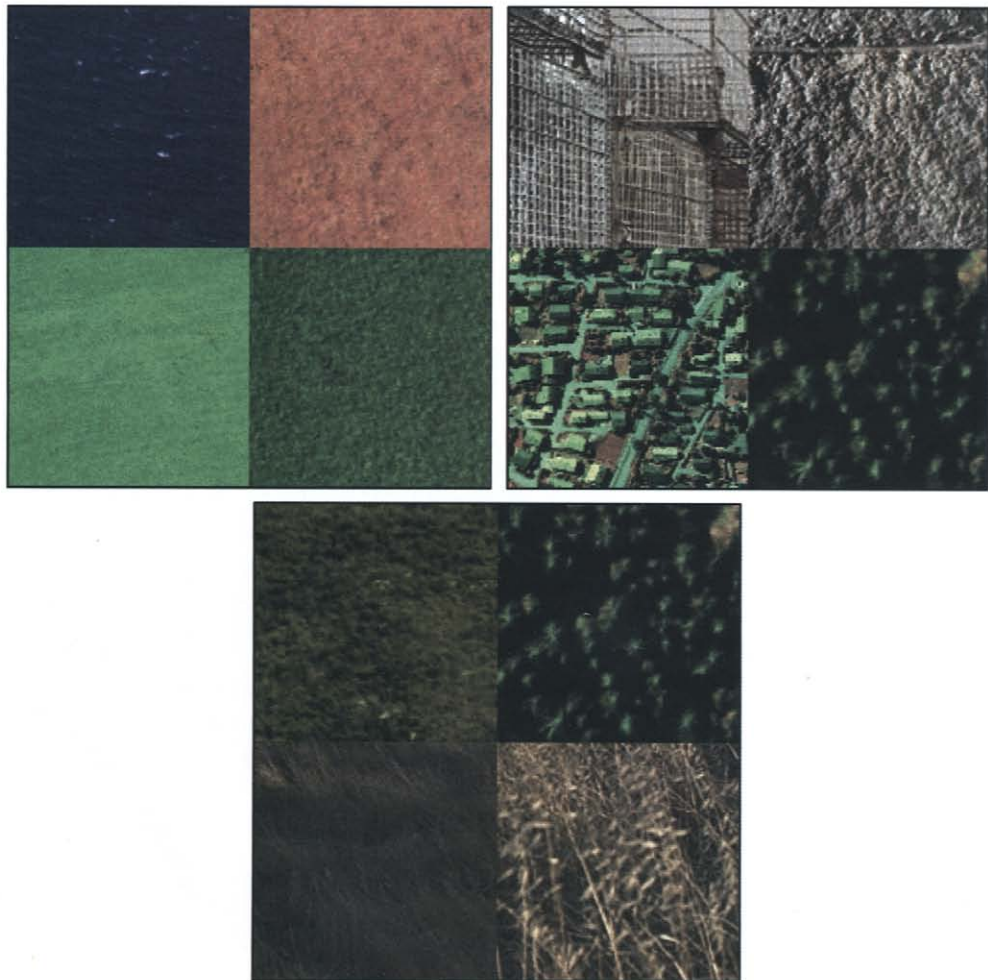


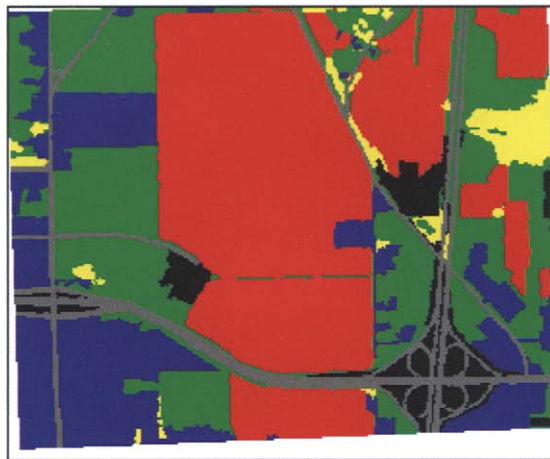
FIGURE 4.8.2 Collection of images; in each there are four clearly distinguishable segments.



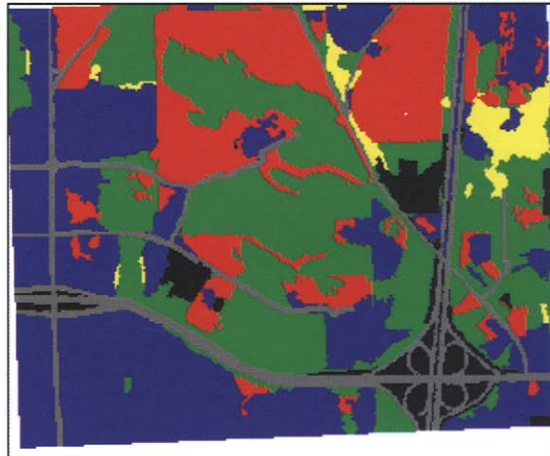
FIGURE 4.8.5 Correct estimation of the vehicle ahead, using the MAP procedure.



FIGURE 4.8.6 Segmentation of other images, using the same Fisher color distance. Top: A segmentation that yields all segments that contain the color white. Bottom: A segmentation that yields all segments that do not contain the color green.



(b)



(d)

FIGURE 4.8.7 Updating old maps using image segmentation. (b) Map of the same area in 1987. (d) Updated map in 1993.

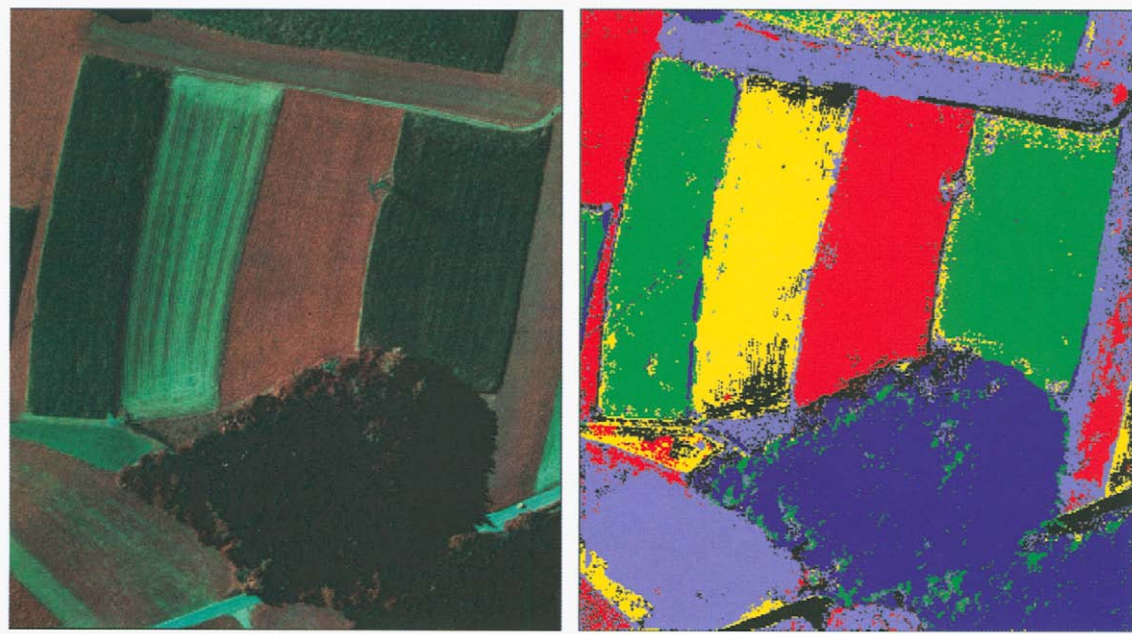


FIGURE 4.8.8 Segmentation of another aerial image, this time of a rural crop field area, using the same texture-based maximum likelihood procedure employed in Fig. 7.

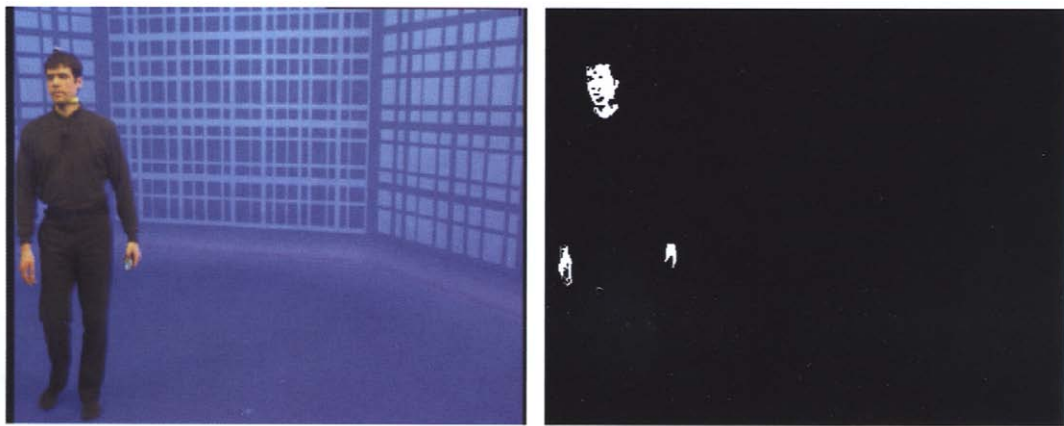


FIGURE 4.11.1 Skin detection based on simple thresholding in the Hue-Saturation components of the HSV color space.